ICEBERG TRACKING FOR SHIP ROUTING

Gisela K. Carvajal and Anders Berg

Chalmers University of Technology, Department of Earth and Space Sciences,
Gothenburg, Sweden; gisela.carvajal@chalmers.se

ABSTRACT

The threat of icebergs can cause major detours from planned ship routes in polar areas, adding extra delays and increasing fuel consumption. For this reason it may be beneficial to incorporate iceberg drift models into near real time ship routing. Here we use a model that implements the vertical distribution of water currents and the Coriolis effect to predict the drift and deterioration of icebergs. Input data include an iceberg concentration product derived from satellite radar data and forecast data of ocean parameters. Icebergs may be modeled with different shapes and sizes, though a standard iceberg is used to predict the average motion of a set of icebergs. The output constitutes a predicted iceberg risk or probability. The use of near-real-time and forecast products aims to contribute to the near-real-time optimization of ship routing in polar areas.

INTRODUCTION

Shipping and other offshore developments have led to increasing demands for reliable iceberg drift forecasts, and new forecast output concerning, for example, calving and small ice mass populations [1-3].

The Canadian Ice Service (CIS) developed an operational model to forecast iceberg drift and deterioration [1]. This model deals with the dynamics and drift of icebergs [4], as well as the deterioration of the icebergs due to various thermal processes and calving.

The present work makes an approximation of the iceberg drift model of [1] that uses near-real-time iceberg concentration data derived from Synthetic Aperture Radar (SAR) to predict the iceberg drifting trajectory. The implemented iceberg model also incorporates forecast data of sea surface parameters aiming for a reliable setting of the ocean conditions in the predicted iceberg trajectories.

METHOD

The equation of the balance of linear momentum which govern the drift of an iceberg can be expressed as [1, 4]:

$$m\left(\frac{d\vec{V}}{dt} + f \times \vec{V}\right) = \tau_a + \tau_w + \tau_c + \tau_i + \tau_t \quad (1)$$

where m and $\vec{V}$ are the mass and velocity of the iceberg, respectively, f is the Coriolis force parameter. To the right side of the equality are different forces due to air drag (τ_a), water stress (τ_w), Coriolis force (τ_c), internal ice stress (τ_i) and the force due to the sea surface tilt (τ_t).

To make the forecast in a simplified way, this work assumes only τ_w and τ_c as main forces governing the iceberg drift.

The force due to the water stress is

$$\tau_w = \frac{1}{2}\rho_w C_w \sum_k A_w(k) \left|\overrightarrow{u_w(k)} - \vec{V}\right| \left(\overrightarrow{u_w(k)} - \vec{V}\right) \quad (2)$$

where ρ_w is the water density [5], C_w is the drag coefficient, A_w is an estimated area of the iceberg [6], and $\overrightarrow{u_w(k)}$ is the water current.

The magnitude of the Coriolis force is given by

$$F_c = 2m\varpi\vec{V}\sin\phi \quad (3)$$

where ϖ is the angular velocity of the Earth and ϕ is the latitude.

From [1] the numerical solution for the iceberg movement is:

$$\frac{d\vec{V}}{dt} = \vec{a}(t,\vec{V}) \quad (4)$$

$$\vec{V}^{i+1} = \vec{V}^i + \Delta t\left(1 - \Delta t\frac{\partial\vec{a}}{\partial\vec{V}}\right) \quad (5)$$

DATA

The data used in this work has been provided by the MyOcean web service[1].

Iceberg product

The “Arctic Ocean - SAR Sea Ice Berg Concentration” product describes the iceberg concentration as number of icebergs counted within 10x10 km grid cells. The product is provided by the Danish Meteorological Institute (DMI). It is derived by applying a Constant False Alarm Rate (CFAR) algorithm on data from SAR satellite sensors. Currently used SAR sensors include the ones on-board Radarsat-2 and Sentinel-1.

Figure 1 shows the geographical locations of the SAR data used in the derivation of the iceberg product presented in this work.

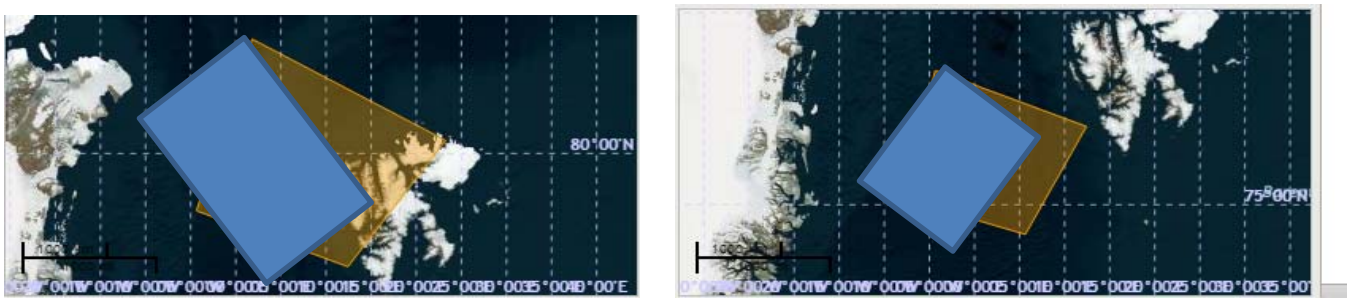

(a) (b)

Figure 1: Examples of geographical locations of SAR images from Sentinel-1 (brown) and Radarsat-2 (blue) used to derive iceberg concentration product.

Figure 2 shows the iceberg locations derived for each SAR image. Although the products were derived from SAR images acquired in the same orbit for each sensor, they are represented in two separated subfigures to zoom out their coverage. Figure 2 (a) shows overlap between the iceberg

[1] http://marine.copernicus.eu/web/69-myocean-interactive-catalogue.php

locations from the two products at the middle of the figure, while in (b) the iceberg overlap is at the western part of the figure.

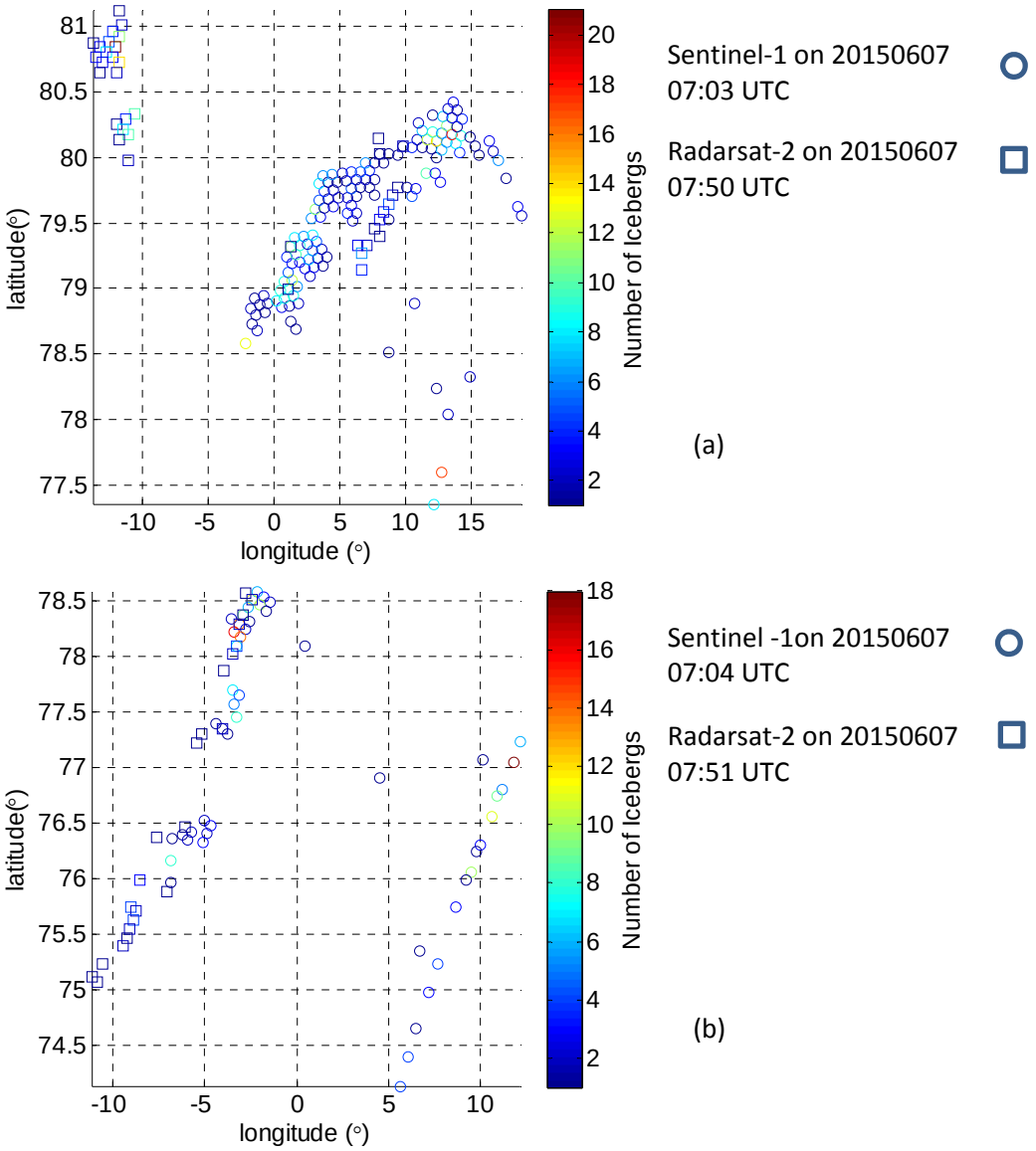

Figure 2: Iceberg concentration within 10x10 km on 7 June 2015 at 07:03, 07:04, 07:50 and 07:51 UTC.

Ocean parameters

The information about currents, temperature and salinity necessary for the computations of the iceberg drift trajectories are derived from the *Global Ocean 1/12° Physics Analysis and Forecast* product. This operational product provides 7 days of 3D global ocean forecasts updated daily.

RESULTS

Predicted iceberg drift

The predictions of the iceberg trajectories were performed by solving the balance equation (1), using modelled ocean parameters and an estimate of the iceberg characteristics. As indicated in the

previous section, the initial location and concentration of the icebergs was given by the iceberg product from DMI.

Figure 3 shows the predictions from the implemented model at intervals of half an hour. Since each iceberg cluster is 10x10 km, it can be seen that the predicted iceberg displacement is generally lower than 3 m/s.

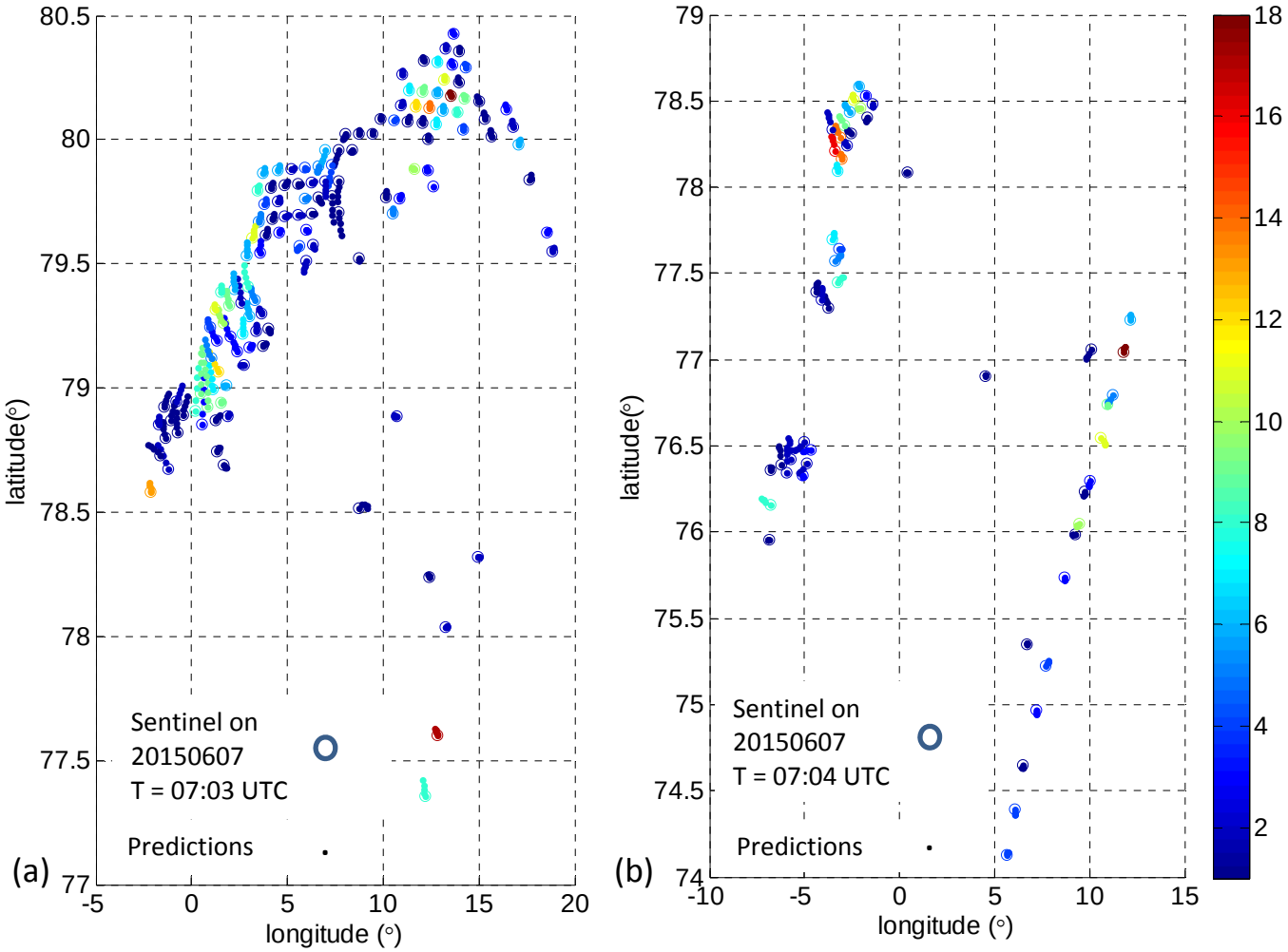

Figure 3: Predicted iceberg drift in a 2 hours interval.

Comparison of reference and predicted trajectories

Figure 4 compares the initial iceberg product with "valid" predictions. The predicted iceberg locations have been fitted to the time on the Radarsat-2 product from the DMI at T_1=07:50, 07:51 UTC. As a first approximation, a predicted location from the Sentinel product at T was considered valid if the maximum distance with the Radarsat-2 product at T_1 was less that about 0.5 degrees in average. Thus, only a subsect of the predicted and the Radarsat-2 iceberg product are shown which correspond to the "unique" iceberg locations with a short distance in the datasets at T_1.

Proximity between predicted and actual iceberg locations indicates promissing results of the model implementation with an offset of 0.23 degrees in Figure 4(a) and of 0.15 degrees in Figure 4(b) . The fact that the shown iceberg predictions were constrained to be close to the data at T_1 makes a

predispositon in the agreement of the results. The main reason for this selection was to expect a common dataset from both products where an iceberg is expected to travel some distance during the 47 minutes of time interval between T and T_1. Nevertheless, the fact that the iceberg concentration products do not include details of the iceberg sizes and distributions in each 10x10 km restricts the validity of the results that can only be assessed by acquiring in-situ data.

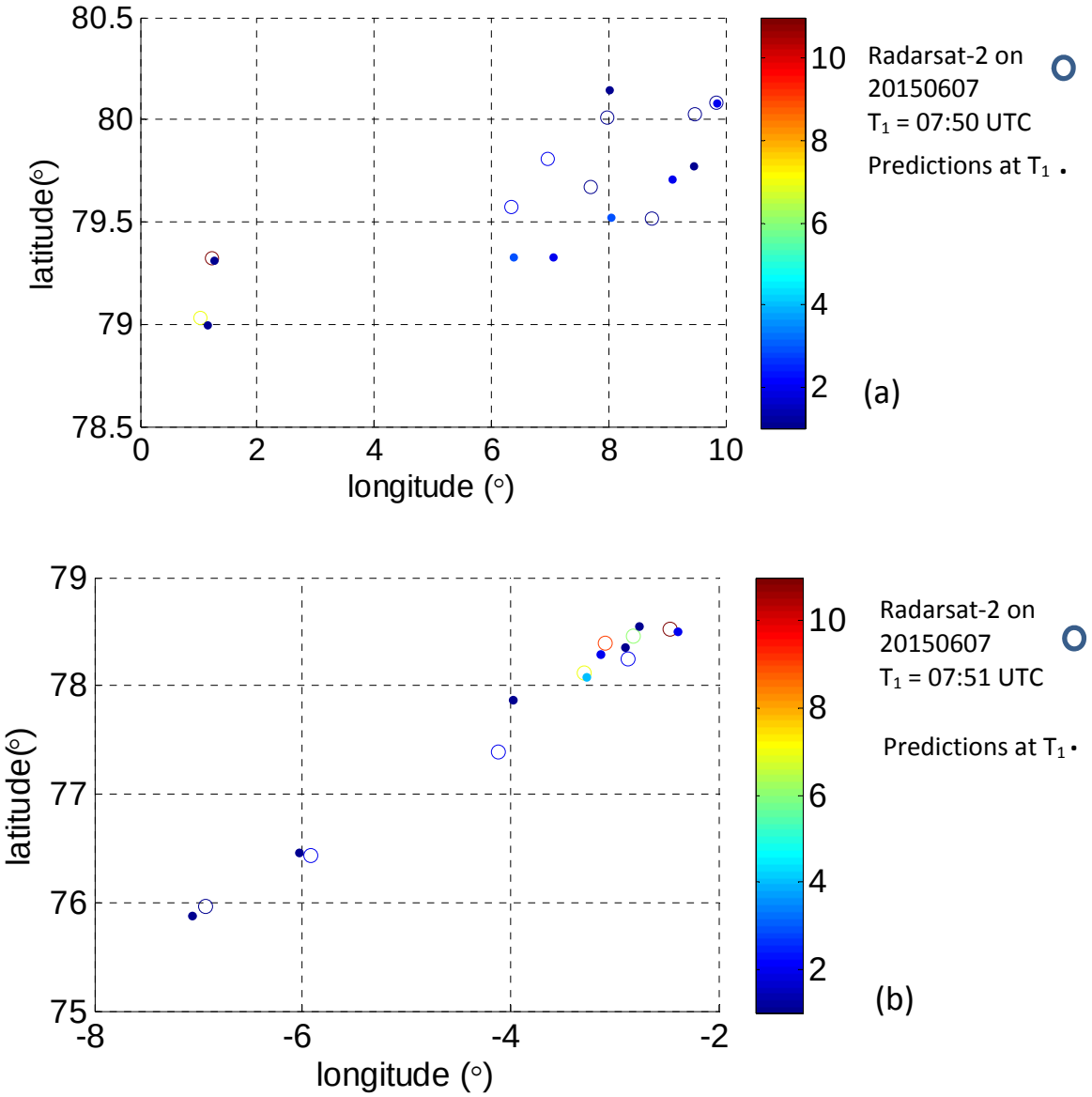

Figure 4: Comparison of initial (T_0) and predicted (T_1) iceberg locations with matching iceberg locations at T_1.

CONCLUSIONS

This work implemented an iceberg drift model using near-real-time iceberg concetration products and forecasted data of ocean parameters. Proximity between predicted and actual iceberg locations indicates promissing results of the model implementation. However, there is a need of in-situ data to assess the validity of the predicted iceberg trajectories to be certain that the results are directly related to measurable drifts from icebergs.

ACKNOWLEDGEMENTS

This work has been sponsored by the *EU 7th framework program* project: "Space-based maritime navigation", Grant agreement no: 607371.

REFERENCES

[1] I. Kubat, M. Sayed, S. B. Savage, and T. Carrieres, "An operational model of iceberg drift," International Journal of Offshore and Polar Engineering, vol. 15, pp. 125-131, 2005.

[2] E. J. Stewart, A. Tiyy, S. E. L. Howell, J. Dawsqn, and D. Draper, "Cruise tourism and sea ice in Canada's Hudson bay Region," Arctic, vol. 63, pp. 57-66, 2010.

[3] R. Ressel, A. Frost, and S. Lehner, "Navigation assistance for ice-infested waters through automatic iceberg detection and ice classification based on TerraSAR-X imagery," in International Archives of the Photogrammetry, Remote Sensing and Spatial Information Sciences - ISPRS Archives, 2015, pp. 1049-1056.

[4] P. Wadhams, Ice in the ocean: Gordon and Breach Science Publishers, 2000.

[5] S. C. McCutcheon, J. L. Martin, and T. O. J. Barnwell, "Water Quality," in Handbook of Hydrology, ed: McGraw-Hill, 1993.

[6] I. S. Hotzel and J. D. Miller, "Icebergs: their physical dimensions and the presentation and application of measured data," Annals of Glaciology, vol. 4, pp. 116-123, 1983.